



Published in final edited form as:

Nat Genet. 2013 May ; 45(5): 495–500. doi:10.1038/ng.2585.

Genomics of *Loa loa*, a *Wolbachia*-free filarial parasite of humans

Christopher A. Desjardins¹, Gustavo C. Cerqueira¹, Jonathan M. Goldberg¹, Julie C. Dunning Hotopp², Brian J. Haas¹, Jeremy Zucker¹, Jose' M.C. Ribeiro⁴, Sakina Saif¹, Joshua Z. Levin¹, Lin Fan¹, Qiandong Zeng¹, Carsten Russ¹, Jennifer R. Wortman¹, Doran L. Fink^{3,*}, Bruce W. Birren¹, and Thomas B. Nutman³

Thomas B. Nutman: tnutman@niaid.nih.gov

¹Broad Institute of MIT and Harvard, Cambridge, MA

²Institute for Genome Science, Department of Microbiology & Immunology, University of Maryland School of Medicine, Baltimore, MD

³Laboratory of Parasitic Diseases, National Institute of Allergy and Infectious Diseases, Bethesda, MD

⁴Laboratory of Malaria and Vector Research, National Institute of Allergy and Infectious Diseases, Bethesda, MD

Abstract

Loa loa, the African eyeworm, is a major filarial pathogen of humans. Unlike most filariae, *Loa loa* does not contain the obligate intracellular *Wolbachia* endosymbiont. We describe the 91.4 Mb genome of *Loa loa*, and the genome of the related filarial parasite *Wuchereria bancrofti*, and predict 14,907 *Loa loa* genes based on microfilarial RNA sequencing. By comparing these genomes to that of another filarial parasite, *Brugia malayi*, and to several other nematode genomes, we demonstrate synteny among filariae but not with non-parasitic nematodes. The *Loa loa* genome encodes many immunologically relevant genes, as well as protein kinases targeted by

Users may view, print, copy, download and text and data- mine the content in such documents, for the purposes of academic research, subject always to the full Conditions of use: http://www.nature.com/authors/editorial_policies/license.html#terms

Correspondence to: Thomas B. Nutman, tnutman@niaid.nih.gov.

* current address: Center for Biologics Evaluation and Research, Food and Drug Administration, Rockville, MD

URLs

Repeat masker, <http://www.repeatmasker.org>; GLU package, <http://code.google.com/p/glu-genetics>; TransposonPSI, <http://transposonpsi.sourceforge.net>; Pristionchus database, <http://www.pristionchus.org>; WormBase, <http://www.wormbase.org>; KinBase database, <http://www.kinase.com>; WormCyc database, <http://wormcyc.broadinstitute.org>.

Accession Codes

All genome assemblies are available in Genbank under the following BioProject identifiers/accession numbers: *L. loa* (PRJNA37757/ADB02000000), *W. bancrofti* (PRJNA37759/ADB01000000), *O. volvulus* (PRJNA37761/ADB01000000), *Wolbachia* of *W. bancrofti* (PRJNA43539/ADHD00000000), and *Wolbachia* of *O. volvulus* (PRJNA43537/ADHE00000000).

Author Contributions

T.B.N., B.W.B. and D.L.F. conceived and designed the project. T.B.N. and D.L.F. provided the samples. J.Z.L., L.F. and C.R. coordinated and/or conducted the sequencing. S.S. assembled the genomes. J.M.G., B.J.H. and Q.Z. annotated the genomes. C.A.D., T.B.N., G.C.C., J.M.G., J.C.D.H., J.Z., D.L.F. and J.M.C.R. analyzed the genomes. C.A.D., T.B.N., G.C.C., J.M.G. and J.C.D.H. wrote the paper. T.B.N., B.W.B., J.R.W. and B.J.H. supervised and coordinated the project.

Competing Financial Interests

Each of the authors declares that they have no competing financial interests

drugs currently approved for humans. Despite lacking *Wolbachia*, *Loa loa* shows no new metabolic synthesis or transport capabilities compared to other filariae. These results suggest that the role played by *Wolbachia* in filarial biology is more subtle than previously thought and reveal marked differences between parasitic and non-parasitic nematodes.

Introduction

Filarial nematodes dwell within the lymphatics and the subcutaneous tissues of up to 170 million people worldwide and are responsible for notable morbidity, disability and socioeconomic loss¹. Although eight filarial species infect humans, only five cause significant pathology -- *Wuchereria bancrofti*, *Brugia malayi*, and *Brugia timori*, the causative agents of lymphatic filariasis; *Onchocerca volvulus*, the causative agent of 'river blindness' or onchocerciasis; and *Loa loa*, the African eyeworm; *L. loa* affects an estimated 13 million people and causes chronic infection most often characterized by localized angioedema (Calabar swelling) and/or subconjunctival migration of adult worms across the eye ("African eyeworm"). Complications of infection include encephalopathy, entrapment neuropathy, glomerulonephritis and endomyocardial fibrosis²; *L. loa* is restricted geographically to equatorial West and Central Africa, where its deerfly vector (*Chrysops* spp.) breeds; *L. loa* microfilariae (L1) are acquired by flies from human blood and subsequently develop into infective larvae (L3) before being reintroduced into a human host during a second blood meal (Supplementary Fig. 1). While *L. loa* is the least well-studied of the pathogenic filariae, it has been gaining prominence of late because of the severe adverse events (encephalopathy and death) associated with ivermectin treatment³ in mass drug administration campaigns in West and Central Africa.

L. loa was targeted for genomic sequencing for two reasons. First, in contrast to other pathogenic filariae, *L. loa* lacks the α -proteobacterial endosymbiont *Wolbachia*. The obligate nature of *Wolbachia* symbiosis in *W. bancrofti*, *B. malayi*, and *O. volvulus* has been inferred by studies in which antibiotics (e.g. doxycycline) that target *Wolbachia* (but not the worm itself) have shown efficacy in treating humans with these infections^{4, 5}. Through genomic analysis, *Wolbachia* have been hypothesized to provide essential metabolic supplementation to their filarial hosts^{6, 7}. The absence of the *Wolbachia* endosymbiont in *L. loa* suggests that either there has been lateral transfer of important bacterially-encoded genes or that the obligate relationship between the endosymbiont and its filarial host is dispensable, at least under certain circumstances. Understanding the comparable adaptations of *L. loa* was considered essential to gain insight into the potential impact of the endosymbiont⁸. Second, as the most neglected of the pathogenic filariae but one gaining increasingly more clinical prominence, understanding the host parasite relationship as it relates to the severe post-treatment reactions typical of both *Wolbachia*-containing and *Wolbachia*-free filarial parasites became of paramount importance.

Thus, we generated a draft genome sequence of *L. loa* generated and produced a refined gene annotation aided by transcriptional data from *L. loa* microfilariae. We also generated draft genome sequences of two of the most pathogenic (and *Wolbachia*-containing) filarial

species, *W. bancrofti* and *O. volvulus*. This approach enabled us to define more comprehensively the genomic differences between *L. loa* and other filarial parasites.

Genome assemblies and repeat content

The nuclear genome of *Loa loa* consists of five autosomes plus a sex chromosome. Using 454 whole genome shotgun sequencing, *L. loa* was sequenced to 20x coverage and assembled into 5774 scaffolds with an N50 of 172 Kb and total size of 91.4 Mb (Table 1). The *W. bancrofti* and *O. volvulus* genomes derived from single adult worms (an unsexed juvenile adult worm for *W. bancrofti* and an adult male worm for *O. volvulus*) were sequenced to 12x and 5x coverage, respectively (Table 1). Because of the low coverage of the *O. volvulus* genome, it was not included in further analysis. While the assembly sizes of the *L. loa* and *B. malayi* genomes are comparable (91.4 Mb versus 93.7 Mb), the scaffold N50 of the *L. loa* genome is almost twice that of *B. malayi*, making the *L. loa* genome assembly the most contiguous assembly of any filarial nematode to date. The filarial genomes differ widely in repeat content (Table 1, Supplementary Tables 1–14, Supplementary Note) with the *L. loa* genome being more repetitive than *W. bancrofti* but less than *B. malayi*.

As nuclear *Wolbachia* transfers (nuwts) have been identified in all *Wolbachia*-colonized and *Wolbachia*-free filarial nematodes examined⁹, we expected to find similar transfers in the *L. loa* genome. However, a BLAST-based search of the assembled *L. loa* genome did not reveal any large transfers of *Wolbachia* DNA. A more sensitive read-based analysis determined that the *L. loa* genome does not have any large, recent transfers (> 500 bp, Supplementary Note). It does however have small, presumably “older”, transfers supporting the hypothesis that *L. loa* was once colonized by *Wolbachia* but subsequently lost its endosymbiont (Supplementary Table 15 and Supplementary Fig. 2). Of the transfers definitively of *Wolbachia* ancestry, and not of possible mitochondrial ancestry, there is no evidence that these are functional in *L. loa* (Supplementary Note).

Gene content and synteny

Initial gene sets were produced for both *L. loa* and *W. bancrofti* based on a combination of gene predictors with refinements to the *L. loa* annotation based on RNA sequence (RNA-Seq) data (see Methods). The final *L. loa* gene set contains 14,907 genes, 70% of which are supported by RNA-Seq (Table 1, Supplementary Tables 16, 17). The *W. bancrofti* genome is predicted to encode 19,327 genes (Table 1, Supplementary Note). The filarial genomes show a high degree of synteny (Figure 1), with 40% and 13% of *L. loa* genes being syntenic relative to *B. malayi* and *W. bancrofti*, respectively. Nearly all syntenic breaks between filarial genomes occur at scaffold ends (Supplementary Fig. 3B), suggesting the percentage is limited by assembly contiguity and the true level of synteny is much higher. When the *L. loa* genome is compared to that of *C. elegans*, orthologs from a single *L. loa* scaffold map predominantly to a single *C. elegans* chromosome (Figure 1). However, only 2% of all *L. loa* genes were syntenic relative to *C. elegans* (Supplementary Fig. 3A), supporting the hypothesis that genome rearrangements during filarial evolution were mostly intra-

chromosomal⁷. An intermediate level of synteny (12%) is seen between *L. loa* and related non-filarial parasite *Ascaris suum* (Supplementary Fig. 3A).

More than half of the genes encoded by the *L. loa* and *W. bancrofti* genomes could be assigned functional categories, PFAM domains, Gene Ontology (GO) terms, and/or Enzyme Commission (EC) numbers (Supplementary Fig. 4, Supplementary Tables 16, 18). Relative to other filarial genomes, the *L. loa* genome is enriched ($p < 0.05$, Fisher's exact test) for numerous domains, including pyridoxamine 5'-phosphate oxidases that synthesize vitamin B (Figure 2; see below). The *L. loa* genome is also enriched for numerous chemoreceptors suggesting that *L. loa* may be capable of more complex interactions with its host environment than other filarial worms (see below; Supplementary Note). An RNA helicase domain involved in viral DNA replication is enriched in the *L. loa* genome; this domain was likely horizontally transferred to the *L. loa* genome from cyclovirus infection (Supplementary Note). While not statistically significant, the *L. loa* genome encodes many more hyaluronidases (6) than the *B. malayi* or *W. bancrofti* genomes (2 each). Hyaluronidases are often involved in tissue penetration and could allow *L. loa* to move more readily through human host tissue, as *L. loa* adults are highly mobile whereas *B. malayi* and *W. bancrofti* adults are commonly tethered to the lymphatic endothelium.

The genome of *W. bancrofti* is enriched ($p < 0.05$, Fisher's exact test) for genes with domains related to cellular adhesion and the extracellular matrix (e.g., cadherins, laminins, and fibronectins). Whether these are important in mediating the fibrosis associated with lymphatic filarial disease (e.g. elephantiasis, lymphedema) in *W. bancrofti* infection¹⁰ or with establishing an anatomical niche within the afferent lymphatics where the adults reside awaits clarification.

Gene products associated with immunologic responses

Each of the filarial parasites interacts with both its definitive mammalian and intermediate arthropod hosts (*Chrysops* spp. in the case of *L. loa*) during its life cycle (Supplementary Fig. 1). The parasite is thought not only to have its own innate immune system to protect itself from microbial pathogens, but also to have evolved mechanisms to exploit and/or subvert host and vector defense mechanisms. Although adaptive immune molecules such as immunoglobulins or Toll-like receptors (TLRs) are absent in *L. loa* and other filarial nematodes, *L. loa*, like other filariae, appears to possess a primordial Toll-related pathway (Supplementary Table 19, Supplementary Note). The innate immune system encoded by the *L. loa* genome also includes C-type lectins, galectins, jacalins, and scavenger receptors; *L. loa* contains a number of lipopolysaccharide binding proteins, proteins implicated in modulating the effects of host bacteria or microbial translocation products. Like *B. malayi*, the *L. loa* (and *W. bancrofti*) genomes do not encode antibacterial peptides described in *C. elegans* and *Ascaris suum*⁷, suggesting that these molecules are either dispensable in filariae or too divergent to detect.

Analysis of *L. loa* genes identified a number of human cytokine and chemokine mimics/antagonists including: genes encoding macrophage migration inhibition (MIF) family signaling molecules, transforming growth factor- β and their receptors, members of the

interleukin (IL)-16 family, an IL-5 receptor antagonist, an interferon regulatory factor, a homolog of suppressor of cytokine signaling (SOCS)-7, and two members of the chemokine-like family (Supplementary Table 19). In addition, the *L. loa* genome encodes 17 serpins and 7 cystatins shown to interfere with antigen processing and presentation to T cells¹¹, 2 indoleamine 2,3 dioxygenase (IDO) genes that encode immunomodulatory proteins implicated in strategies of immune subversion, and a number of the Wnt family of developmental regulators that typically modulate immune activation. The *L. loa* genome encodes proteins that have sequences similar to human autoantigens (Supplementary Note). Although some of these can also be found in the other filariae, the slight expansion of these in *L. loa* suggests that antibodies induced by *L. loa* infection may be more autoreactive than those induced by other parasites.

Protein kinases

In addition to elucidating host-pathogen interactions, pathogen genomes can be evaluated for potential drug targets such as protein kinases. We therefore annotated protein kinases in the *L. loa* genome and compared them to those in other nematode genomes (Supplementary Tables 20–23, Supplementary Fig. 5). Numerous differences were observed between filarial and non-parasitic nematode kinases, particularly regarding meiosis. The widely-conserved TTK kinase (Mps1), which plays a key role in eukaryotic meiosis¹², is present in *L. loa* and absent in *C. elegans*. By contrast, filarial nematodes lack the nearly universally conserved RAD53-family kinase *chk-2*, which is present in *C. elegans*. In most eukaryotes RAD53 is involved in initiating cell-cycle arrest when DNA damage is detected but in *C. elegans* is essential for chromosome synapsis and nuclear rearrangement during meiosis¹³. This reciprocal difference suggests that meiosis in filarial parasites may be regulated in a manner more like typical eukaryotes than *C. elegans* (Supplementary Note). Six *L. loa* protein kinases are orthologous to targets of drugs currently approved for humans (Supplementary Table 23), including the tyrosine kinase inhibitor imatinib that has been shown to kill schistosomes¹⁴ and *Brugia* parasites of all stages at concentrations ranging from 5 to 50 μM (unpublished data). Therefore repurposing already approved drugs that target these kinases may be promising in treating filarial (and other helminth) infections¹⁵.

Nematode phylogenomics

To examine the evolution of filarial parasites in the context of other nematodes, we estimated a phylogeny from 921 single copy core orthologs across nine nematode genomes using maximum likelihood, parsimony, and Bayesian methods. All methods converged on a single topology with 100% support (either bootstrap values or posterior probabilities) at all nodes (Figure 3). This phylogeny indicates that *Meloidogyne hapla* occupies a position basal to a clade of Rhabdina (i.e; *C. elegans*, *C. briggsae*, and *Pristionchus pacificus*) and to the Spirurina (i.e. filarial worms and *Ascaris suum*). While these results contrast with previous studies based on ribosomal subunits that placed *M. hapla* closer to Rhabdina than the filarial worms^{16, 17}, our analysis utilized a larger gene set and has higher nodal support values.

Relative to the genomes of non-parasitic nematodes, numerous orthologs were identified as unique to the filarial parasites (Figure 3). Proteins encoded by the filarial genomes show enrichment of immunogenic domains such as extracellular and cell adhesion domains, and in a metabolic context are enriched for trehalase domains involved in trehalose degradation ($q < 0.05$, Fisher's exact test; Supplementary Fig. 6). Trehalose is known to be involved in the protection of nematodes from environmental stress¹⁸ and could potentially play a key role in filarial survival. Trehalose levels have also been associated with increased lifespan in *C. elegans*¹⁹ and might support the idea that an increased use of trehalose by filarial nematodes could be related to their relatively long lifespan.

The filarial genomes lack a wide array of seven transmembrane G-protein-coupled chemoreceptors (7 TM GPCRs; Supplementary Fig. 6). Profiling of 7 TM GPCRs revealed a pattern of progressive loss of many families in the transition from non-parasitic to parasitic lifestyles (Figure 4). For example, filarial nematodes and *T. spiralis* completely lack the Str superfamily, including *odr-10*, known to be involved in detection of volatiles²⁰, and Kin-29, a protein kinase that regulates Str expression in *C. elegans*²¹. If the Str superfamily is more broadly involved in odorant detection, this could explain why these molecules are lacking in filarial nematodes and *T. spiralis* parasites that only live in aqueous environments, while they are retained in *A. suum* and *M. hapla*, which are exposed to volatiles in part of their life cycle. Only the Srab, Srx, Srsx, and Srw families were conserved across all nematodes, suggesting that these GPCRs mediate vital nematode functions.

Filarial genomes are also depleted in both soluble and receptor guanylate cyclases – these genes are involved in the regulation of environmental sensing and complex sensory integration functions (Figure 4). However, *gcy-35* and *gcy-36*, which are involved in the detection of molecular oxygen in solution²², are encoded in the filarial genomes. Protein kinase profiling revealed 18 receptor guanylate cyclases which are present in *C. elegans* but not in filarial worms, including environmental sensors *gcy-14* and *gcy-22* (Supplementary Table 23). Depletion of these and other kinases involved in olfactory and gustatory sensing, including kin-29, suggests that the environments of filarial nematodes are less complex in terms of chemosensory inputs than are those inhabited by non-parasitic nematodes (Supplementary Note). The *L. loa* genome does, however, encode significantly more chemoreceptors than do other filarial nematodes ($p < 0.05$, Fisher's exact test), which may be related to the increased mobility of *L. loa* adult worms.

Phylogenetic profiling of metabolism

Previous genomic analysis identified five biosynthetic pathways (heme, riboflavin, FAD, glutathione and nucleotides) present in *Wolbachia* but missing from its relatives, e.g; *Rickettsia*. These *Wolbachia*-encoded pathways were hypothesized to provide metabolites needed by their filarial hosts⁶. As *L. loa* lacks *Wolbachia*, it was theorized that the *L. loa* genome must encode genes to replace these pathways, potentially laterally transferred from *Wolbachia* to an ancestor of *L. loa*. However, no transfers relating to these metabolic functions were apparent (see above). Thus, we generated complete metabolic pathway reconstructions for nine nematode and four *Wolbachia* genomes (Table 2, Supplementary Tables 24, 25) to determine how *L. loa* acquires these metabolites and placed the results in

an evolutionary context. Unexpectedly, none of the five “complementary” pathways differ between *L. loa* and the other filarial nematodes, calling into question the role of these pathways in filarial-*Wolbachia* symbiosis.

Furthermore, in only two pathways (heme and nucleotide synthesis) did the filarial genomes differ from the other nematodes. The FAD and glutathione pathways are complete in all nematode genomes, while the riboflavin pathway is missing from all nematode genomes. The heme biosynthesis pathway, previously reported to be absent in *B. malayi*⁷, is missing from not only the filarial worms but from all nematode genomes characterized to date. Experimental work on *C. elegans* (also *Wolbachia*-free) has shown that it cannot synthesize heme *de novo*²³; *B. malayi* has been previously noted as having a single member of the heme synthesis pathway, ferrochelatase (an enzyme that catalyzes the last step in heme synthesis⁷ [Supplementary Note]). The gene encoding ferrochelatase is also present in the *L. loa* and *W. bancrofti* genomes, but absent in all other nematode genomes, including *A. suum*. It is possible that this gene in filarial nematodes is not involved in heme synthesis, but rather in an alternate, unknown pathway.

Like *B. malayi*, both *L. loa* and *W. bancrofti* lack the ability to synthesize nucleotides *de novo*. All three filarial genomes lack the majority of the proteins involved in the purine synthesis pathway as well as the first enzyme involved in the pyrimidine synthesis pathway (Table 2, Supplementary Table 24). Other nematodes have also lost portions of these pathways; the purine synthesis pathway has been largely lost in *P. pacificus* and *M. hapla*, while the first two enzymes in the pyrimidine synthesis pathway have been lost in *T. spiralis*. These multiple and likely independent losses could underscore a general flexibility in the need for *de novo* nucleotide synthesis in nematodes. All nematodes, including the filariae, have complete sets of purine and pyrimidine interconversion pathways (Supplementary Table 24), implying that they could generate all necessary nucleotides from a single purine and pyrimidine source, a concept supported by experimental data in *B. malayi*²⁴. Filarial genomes do encode two purine-specific 5' nucleotidases for salvage whereas all other nematodes encode only one; the extra copy in the filariae appears to arise from a single gene duplication event and diverged significantly from the ancestral gene (Supplementary Fig. 7). Additionally, we profiled known nematode and *Wolbachia* transporters linked to these pathways, and found no evidence of differences between filarial and non-filarial nematodes nor among *Wolbachia* endosymbionts (Supplementary Note and Supplementary Fig. 8). Given the uniformity of these pathways across nematodes and the apparent lack of any related transfers of *Wolbachia* DNA to the *L. loa* genome, it is likely that the symbiotic role played by *Wolbachia* in filarial nematodes either lies outside these pathways or involves more subtle metabolic supplementation rather than the wholesale provision of unproduced metabolites.

The only metabolic pathway found to differ in gene content between *L. loa* and other nematodes with sequenced genomes is vitamin B6 synthesis and salvage. Most nematode genomes encode single copies of the two enzymes involved in vitamin B6 salvage, while the *L. loa* genome encodes five copies of the second enzyme, pyridoxal 5'-phosphate synthase (Supplementary Note). This pathway also differed among *Wolbachia* genomes. While both of the insect *Wolbachia* genomes also encoded two genes involved in the synthesis of

vitamin B6 (*pdxJ* and *pdxK*), neither of the filarial *Wolbachia* genomes did (the difference between *wBm* and *wMel* having been noted previously⁶). If the filarial *Wolbachia* endosymbionts need to acquire vitamin B6 exogenously, this could explain a metabolic need of *Wolbachia* fulfilled by the nematode. However, with that hypothesis in mind, it is unclear why *L. loa*, the one pathogenic filarial nematode without *Wolbachia*, would encode a greater number of vitamin B6 salvage genes than either *B. malayi* or *W. bancrofti*. We could not exclude differences in pyroxidine transporters as no orthologs of known transporters could be identified in either nematode or *Wolbachia* genomes (Supplementary Note).

Conclusion

The study of some of the nematode genomes has already provided great insight into the genomic structure, biology and evolution of this major division of nematode parasites. With the release of the genome of *L. loa*, a human pathogen and parasitic nematode that does not contain *Wolbachia*, we have been able provide surprising insights into the dispensability of this endosymbiont that deepen the mystery surrounding the “essential nature” of *Wolbachia* for many filarial worms.

Through large-scale genomic comparisons within the phylum Nematoda, we have not only been able to define molecules and pathways that are either *Loa loa*- or filaria-specific but also, by comparison with the non-parasitic nematodes (e.g; *C. elegans*), we have gained a first glimpse into the nature of parasitism itself. Moreover, this effort has identified new targets for intervention that should aid programs aimed at control and elimination of these important but neglected parasites.

Online Methods

Sequencing and Assembly

For *L. loa*, 5×10^5 microfilariae (mf) were purified during a therapeutic apheresis from a patient with loiasis infected in Cameroon seen at the NIH under protocol 88-I-83 (NCT00001230). A single unfertilized adult *W. bancrofti* worm was obtained under ultrasonic guidance (as part of protocol NCT00339417) in Tienegabougou, Mali. A single adult *O. volvulus* male was isolated from a surgically-removed subcutaneous nodule in Ecuador after collagenase digestion. Genomic DNA for all samples was prepared using the Qiagen genomic DNA kit (Qiagen, Gaithersburg, MD). DNA obtained from *W. bancrofti* and *O. volvulus* was amplified using the Qiagen Repli-g midi kit. For *L. loa*, *W. bancrofti*, and *O. volvulus*, approximately 50, 10, and 5 ug of DNA was used for genomic sequencing, respectively. For *L. loa*, 454 shotgun fragment and 3Kb jumping sequencing libraries were prepared and sequenced as previously described²⁵. Only fragment libraries were constructed for *W. bancrofti* and *O. volvulus*. Assemblies were then generated using Newbler version 2.1 (Roche 454 Life Sciences). Given the overall low coverage of the *W. bancrofti* and *O. volvulus* assemblies (5–12x), no bias normalization was done for the whole-genome amplified sequence data. Also for the *W. bancrofti* and *O. volvulus* assemblies, contigs were screened by BLASTing against Genbank’s non-redundant nucleotide database (NT) using a cutoff of $1e-25$ and minimum match length of 100 bp, and all contigs where the top match was to *Wolbachia* were removed. Any contigs remaining in the nematode assembly that had

secondary matches to *Wolbachia* were screened manually to ensure that no large chimeric contigs had been generated and retained. Unassembled reads were also screened for *Wolbachia* sequence using the same BLAST parameters and database. Unassembled reads identified as *Wolbachia*, along with reads underlying the contigs identified as *Wolbachia*, were assembled together using Newbler version 2.1 to generate the *Wolbachia* genome assemblies.

Repeat Content Analysis

Repeat content was identified using RepeatScout²⁶ followed by RepeatMasker using both nematode repeats from RepBase v17.06²⁷ and the output from RepeatScout. Only hits with Smith-Waterman score above 250 were maintained. Additional repeats were then identified based on abnormally high read coverage in the genome assemblies, utilizing genome sequence scanning with hysteresis triggering. Positions with read depth 20 times the mode of the read depth distribution switched the “collapsed reads” state to ON during the scanning process, while positions with read depth lower than 10 times the mode switched the “collapsed reads” state to OFF. Only regions longer than 100 nucleotides were reported. Read mapping was performed by runMapping application of the Newbler suite²⁸. The output was converted to SAM file format by seq.Newbler2SAM option of GLU package. Only the best alignment of each read was kept. Read depth was calculated by the genomeCoverageBed program of BEDTools suite²⁹.

RNA Sequencing

RNA was prepared from one million *L. loa* mf purified from the blood of a patient. Under liquid nitrogen, mf were disrupted by a stainless steel piston apparatus. Total RNA was extracted using the RNeasy Kit (Qiagen, Valencia, CA, USA). A non-strand-specific cDNA library for Illumina paired-end sequencing was prepared from ~37 ng of total RNA as previously described³⁰ with the following modifications. RNA was treated with Turbo DNase (Ambion, TX) and fragmented by heating at 80 °C for 3 min in 1x fragmentation buffer (Affymetrix, CA) before cDNA synthesis. Sequencing adapter ligation was performed using 4,000 units T4 DNA ligase (New England Biolabs, MA) at 16°C overnight. Following adapter ligation the resulting library was cleaned, size selected twice using 0.7x volumes of Ampure beads (Beckman Coulter Genomics, MA), enriched using 18 cycles of PCR, and cleaned using 0.7x volumes of Ampure beads (Beckman Coulter Genomics, MA). The resulting Illumina sequencing library was sequenced with 76 base paired-end reads on an Illumina GAII instrument (v1.8 analysis pipeline) following the manufacturer’s recommendations (Illumina, CA).

Identification of transfers (nuwts)

An initial search of the *Wolbachia* of *B. malayi* genome against the *L. loa* genome was done using BLASTN with a cutoff of $1e^{-5}$. After this assembly-based search, nuclear *Wolbachia* transfers (nuwts) were identified through a screen of the *L. loa* sequencing reads as being >80% identical to *Wolbachia* sequences over 50% of the read. Searches were refined to examine reads with >50 bp match to *Wolbachia* and were manually curated to remove spurious matches that had a nematode ancestry. Reads matching the bacterial rRNA were

removed as they could arise from any bacterial genome that might be contaminating the sample. Regions of homology <50 bp were included if they were detected through analysis of an adjacent region with homology over >50 bp. All of the reads containing nuwts were mapped back to the *L. loa* genome to identify the consensus sequence and the relationship confirmed using BLASTN to NT. Phylogenetic analysis was conducted on nucleotide sequences of predicted nuwts using RAxML³⁰.

Annotation

Genes for both *L. loa* and *W. bancrofti* were predicted using a combination of *ab initio* gene prediction tools as previously described³¹. We also used TBLASTN to search the genome assembly against protein sequences of the following species: *C. elegans*, *C. briggsae*, *Schistosoma mansoni*, *S. japonicum*, and *B. malayi* (downloaded from Genbank on February 16, 2010). The top BLAST hits are used to construct GeneWise³² gene models. In addition, we generated gene models using available EST data from *L. Loa*, *W. bancrofti*, *O. volvulus*, and *B. malayi* (downloaded from GenBank on December 2, 2009). All of these models were used as input into EVM³³ to generate combined gene predictions. To incorporate the *L. loa* RNA-Seq data, we aligned all RNA-Seq reads to the *L. loa* genome using BLAT³⁴. Next, we use the Inchworm module of the Trinity package³⁵ with default settings in genome-guided mode to assemble the reads into EST-like transcripts. These transcripts along with the models from EVM into PASA³³ were used for gene model improvement. Gene sets were subsequently filtered to remove repeats, including genes overlapping rRNA, tRNA, or output from RepeatScout²⁶ or TransposonPSI. Every annotated gene was given a locus ID of the form LOAG_##### (*L. loa*) or WUBG_##### (*W. bancrofti*). Pfam domains within each gene were identified using Hmmer3³⁶, while gene ontology terms were assigned using BLAST2GO³⁷. Secretion signals and transmembrane domains were identified using SignalP 4.0³⁸ and TmHm³⁹, respectively. Core eukaryotic genes were identified using CEGMA⁴⁰.

Identification of Fragmented Genes

Fragmented *W. bancrofti* genes were associated to their putative intact orthologs in *L. loa* or *B. malayi* by unidirectional BLAST of *W. bancrofti* peptides against peptides from the reference genome (*L. loa* or *B. malayi*); *W. bancrofti* proteins with less than 80% similarity to the reference, based on query length, and an e-value higher than 1×10^{-10} were disregarded. A gene was considered fragmented if its length in *W. bancrofti* was at least 50% shorter than its respective ortholog. The number of reference genome orthologs with multiple assigned fragments in *W. bancrofti* was then used to extrapolate a corrected gene count for *W. bancrofti*. An identical analysis was done for *L. loa* genes by comparison to *B. malayi*.

Synten Analysis

Whole genome alignments of *C. elegans*, *B. malayi* and *W. bancrofti* against *L. loa* were performed by progressive Mauve⁴¹ with default parameters. The extent of the alignment between a pair of sequences was defined as the length spanning all their respective colinear blocks. For each comparison, chromosomes or scaffolds having the longest alignment against *L. loa* scaffold number 4 (100 scaffolds from *W. bancrofti*, 30 scaffolds from *B.*

malayi and *C. elegans* chromosome III) were selected for visualization. For the systematic evaluation of synteny, pairwise syntenic blocks between the genomes of *L. loa*, *C. elegans*, *B. malayi* and *W. bancrofti* were defined by DAGchainer⁴² with minimum numbers of colinear genes set to 3.

Gene Clustering and Phylogenetic Analysis

We built a comparative set of genomes including those sequenced in this study and *Pristionchus pacificus* (from www.pristionchus.org), *Caenorhabditis elegans* (release 224 from WormBase), *C. briggsae* (CAAC00000000), *Meloidgyne hapla* (from www.pngg.org), *Brugia malayi* (release 230 from WormBase), *Ascaris suum* (published release from WormBase), and *Trichinella spiralis* (ABIR00000000). Genes were clustered using OrthoMCL with a Markov inflation index of 1.5 and a maximum e-value of 1×10^{-5} ⁴³. Amino acid sequences of orthologs present as single copies in all genomes were aligned using MUSCLE⁴⁴ and concatenated. We then estimated phylogenies from this dataset using three methods. Parsimony bootstrapping analysis was conducted using PAUP⁴⁵ using unweighted characters and 1,000 bootstrap replicates. For maximum likelihood analysis, we first selected the JG model⁴⁶ using ModelGenerator⁴⁷, and then used the PROTCATJG model in RAxML³⁰ with 1,000 bootstrap replicates. For Bayesian analysis, we used MrBayes⁴⁸ with a mixed amino acid model and gamma distributed rates. We ran the analysis with 1 chain for 1 million generations, sampling every 500 generations, and discarding the first 25% of samples as burn-in. Enrichment analyses were conducted using Fisher's exact test and multiple comparisons were corrected using false discovery rate⁴⁹.

Kinase Classification

Initial sets of protein kinases were identified by orthology with annotated *C. elegans* kinases. Kinases without orthologs were identified in a search of the proteome against a protein kinase HMM derived from an alignment of *Dictyostelium* protein kinases⁵⁰ using a cutoff score of -66. Low-scoring sequences were additionally screened for conservation of known protein kinase sequence motifs. All protein kinases were classified using a controlled vocabulary^{51, 52}, and classifications of filarial kinases with *C. elegans* orthologs were mapped from the curated set from the KinBase database. Kinases without orthologs in *C. elegans* were searched against the curated set using BLAST and classified if the top three hits agreed. Orthology across all nematodes was then used to identify potentially missed kinases and ensure consistent classification.

Metabolic Reconstruction

In addition to the nine nematode genomes listed above, we utilized three additional *Wolbachia* genomes from *B. malayi* (AE017321), *Drosophila melanogaster* (AE017196) and *Culex pipiens* (AM999887). Metabolic pathways were characterized using Pathway Tools⁵³. Metabolic reconstruction was performed using EFICAz2⁵⁴ to assign Enzyme Commission (EC) numbers for each enzyme. EC numbers and gene names were used as input to the Pathologic software⁵⁵ with transport-identification-parser and pathway-hole-filler options set to assign MetaCyc⁵⁶ pathways for each organism. The full set of metabolic pathways for each genome are available at the WormCyc database.

Supplementary Material

Refer to Web version on PubMed Central for supplementary material.

Acknowledgements

We thank members of the Broad Institute Genomics Platform for sequencing and Daniel Neafsey for comments on the manuscript. This project has been funded in part with funds from the National Institute of Allergy and Infectious Diseases, National Institutes of Health, Department of Health and Human Services, under Contract No.:HHSN272200900018C and by the Division of Intramural Research, National Institute of Allergy and Infectious Diseases, National Institutes of Health. J.C.D.H. is funded by the National Institutes of Health Director's New Innovator Award Program (1-DP2-OD007372).

References

1. Hotez PJ, et al. Control of neglected tropical diseases. *N. Engl. J. Med.* 2007; 357:1018–1027. [PubMed: 17804846]
2. Klion, AD.; Nutman, TB. Tropical Infectious Diseases: Principles, Pathogens and Practice. Guerrant, RL.; Walker, DH.; Weller, PF., editors. Churchill Livingstone; 2011. p. 735-740.
3. Gardon J, et al. Serious reactions after mass treatment of onchocerciasis with ivermectin in an area endemic for *Loa loa* infection. *Lancet.* 1997; 350:18–22. [PubMed: 9217715]
4. Taylor MJ, Hoerauf A, Bockarie M. Lymphatic filariasis and onchocerciasis. *Lancet.* 2010; 376:1175–1185. [PubMed: 20739055]
5. Coulibaly YI, et al. A randomized trial of doxycycline for *Mansonella perstans* infection. *N. Engl. J. Med.* 2009; 361:1448–1458. [PubMed: 19812401]
6. Foster J, et al. The *Wolbachia* genome of *Brugia malayi*: endosymbiont evolution within a human pathogenic nematode. *PLoS Biol.* 2005; 3:e121. [PubMed: 15780005]
7. Ghedin E, et al. Draft genome of the filarial nematode parasite *Brugia malayi*. *Science.* 2007; 317:1756–1760. [PubMed: 17885136]
8. Saint Andre A, et al. The role of endosymbiotic *Wolbachia* bacteria in the pathogenesis of river blindness. *Science.* 2002; 295:1892–1895. [PubMed: 11884755]
9. Dunning Hotopp JC. Horizontal gene transfer between bacteria and animals. *Trends Genet.* 2011; 27:157–163. [PubMed: 21334091]
10. Anuradha R, et al. Altered circulating levels of matrix metalloproteinases and inhibitors associated with elevated type 2 cytokines in lymphatic filarial disease. *PLoS Negl. Trop. Dis.* 2012; 6:e1681. [PubMed: 22679524]
11. Hartmann S, Lucius R. Modulation of host immune responses by nematode cystatins. *Int. J. Parasitol.* 2003; 33:1291–1302. [PubMed: 13678644]
12. Gilliland WD, et al. The multiple roles of *mps1* in *Drosophila* female meiosis. *PLoS Genet.* 2007; 3:e113. [PubMed: 17630834]
13. Meier B, Ahmed S. Checkpoints: chromosome pairing takes an unexpected twist. *Curr. Biol.* 2001; 11:R865–R868. [PubMed: 11696343]
14. Beckmann S, Grevelding CG. Imatinib has a fatal impact on morphology, pairing stability and survival of adult *Schistosoma mansoni* in vitro. *Int. J. Parasitol.* 2010; 40:521–526. [PubMed: 20149792]
15. Dissous C, Grevelding CG. Piggy-backing the concept of cancer drugs for schistosomiasis treatment: a tangible perspective? . *Trends Parasitol.* 2011; 27:59–66. [PubMed: 20920890]
16. Meldal BH, et al. An improved molecular phylogeny of the Nematoda with special emphasis on marine taxa. *Mol. Phylogenet. Evol.* 2007; 42:622–636. [PubMed: 17084644]
17. Blaxter ML, et al. A molecular evolutionary framework for the phylum Nematoda. *Nature.* 1998; 392:71–75. [PubMed: 9510248]
18. Pellerone FI, et al. Trehalose metabolism genes in *Caenorhabditis elegans* and filarial nematodes. *Int. J. Parasitol.* 2003; 33:1195–1206. [PubMed: 13678635]

19. Honda Y, Tanaka M, Honda S. Trehalose extends longevity in the nematode *Caenorhabditis elegans*. *Aging Cell*. 2010; 9:558–569. [PubMed: 20477758]
20. Sengupta P, Chou JH, Bargmann CI. odr-10 encodes a seven transmembrane domain olfactory receptor required for responses to the odorant diacetyl. *Cell*. 1996; 84:899–909. [PubMed: 8601313]
21. van der Linden AM, et al. The EGL-4 PKG acts with KIN-29 salt-inducible kinase and protein kinase A to regulate chemoreceptor gene expression and sensory behaviors in *Caenorhabditis elegans*. *Genetics*. 2008; 180:1475–1491. [PubMed: 18832350]
22. Zimmer M, et al. Neurons detect increases and decreases in oxygen levels using distinct guanylate cyclases. *Neuron*. 2009; 61:865–879. [PubMed: 19323996]
23. Rao AU, Carta LK, Lesuisse E, Hamza I. Lack of heme synthesis in a free-living eukaryote. *Proc. Natl. Acad. Sci. USA*. 2005; 102:4270–4275. [PubMed: 15767563]
24. Rajan TV. Exogenous nucleosides are required for the morphogenesis of the human filarial parasite *Brugia malayi*. *J. Parasitol.* 2004; 90:1184–1185. [PubMed: 15562627]
25. Lennon NJ, et al. A scalable, fully automated process for construction of sequence-ready barcoded libraries for 454. *Genome Biol*. 2010; 11:R15. [PubMed: 20137071]
26. Price AL, Jones NC, Pevzner PA. De novo identification of repeat families in large genomes. *Bioinformatics*. 2005; 21(Suppl. 1):351–358.
27. Jurka J, et al. Repbase Update, a database of eukaryotic repetitive elements. *Cytogenet. Genome Res*. 2005; 110:462–467. [PubMed: 16093699]
28. Margulies M, et al. Genome sequencing in microfabricated high-density picolitre reactors. *Nature*. 2005; 437:376–380. [PubMed: 16056220]
29. Quinlan AR, Hall IM. BEDTools: a flexible suite of utilities for comparing genomic features. *Bioinformatics*. 2010; 26:841–842. [PubMed: 20110278]
30. Stamatakis A. RAxML-VI-HPC: maximum likelihood-based phylogenetic analyses with thousands of taxa and mixed models. *Bioinformatics*. 2006; 22:2688–2690. [PubMed: 16928733]
31. Haas BJ, Zeng Q, Pearson MD, Cuomo CA, Wortman JR. Approaches to Fungal Genome Annotation. 2011; 2:118–141.
32. Birney E, Clamp M, Durbin R. GeneWise and Genomewise. *Genome Res*. 2004; 14:988–995. [PubMed: 15123596]
33. Haas BJ, et al. Automated eukaryotic gene structure annotation using EVIDENCEModeler and the Program to Assemble Spliced Alignments. *Genome Biol*. 2008; 9:R7. [PubMed: 18190707]
34. Kent WJ. BLAT--the BLAST-like alignment tool. *Genome Res*. 2002; 12:656–664. [PubMed: 11932250]
35. Grabherr MG, et al. Full-length transcriptome assembly from RNA-Seq data without a reference genome. *Nat. Biotechnol*. 2011; 29:644–652. [PubMed: 21572440]
36. Eddy SR. Accelerated Profile HMM Searches. *PLoS Comput. Biol*. 2011; 7:e1002195. [PubMed: 22039361]
37. Conesa A, et al. Blast2GO: a universal tool for annotation, visualization and analysis in functional genomics research. *Bioinformatics*. 2005; 21:3674–3676. [PubMed: 16081474]
38. Petersen TN, Brunak S, von Heijne G, Nielsen H. SignalP 4.0: discriminating signal peptides from transmembrane regions. *Nat. Methods*. 2011; 8:785–786. [PubMed: 21959131]
39. Krogh A, Larsson B, von Heijne G, Sonnhammer EL. Predicting transmembrane protein topology with a hidden Markov model: application to complete genomes. *J. Mol. Biol*. 2001; 305:567–580. [PubMed: 11152613]
40. Parra G, Bradnam K, Korf I. CEGMA: a pipeline to accurately annotate core genes in eukaryotic genomes. *Bioinformatics*. 2007; 23:1061–1067. [PubMed: 17332020]
41. Darling AE, Mau B, Perna NT. progressiveMauve: multiple genome alignment with gene gain, loss and rearrangement. *PLoS One*. 2010; 5:e11147. [PubMed: 20593022]
42. Haas BJ, Delcher AL, Wortman JR, Salzberg SL. DAGchainer: a tool for mining segmental genome duplications and synteny. *Bioinformatics*. 2004; 20:3643–3646. [PubMed: 15247098]
43. Li L, Stoekert CJ Jr, Roos DS. OrthoMCL: identification of ortholog groups for eukaryotic genomes. *Genome Res*. 2003; 13:2178–2189. [PubMed: 12952885]

44. Edgar RC. MUSCLE: multiple sequence alignment with high accuracy and high throughput. *Nucleic Acids Res.* 2004; 32:1792–1797. [PubMed: 15034147]
45. PAUP*. Phylogenetic Analysis Using Parsimony (*and Other Methods). v. 4.0b10. Sinauer Associates; Sunderland, Massachusetts:
46. Le SQ, Gascuel O. An improved general amino acid replacement matrix. *Mol. Biol. Evol.* 2008; 25:1307–1320. [PubMed: 18367465]
47. Keane TM, Creevey CJ, Pentony MM, Naughton TJ, McLnerney JO. Assessment of methods for amino acid matrix selection and their use on empirical data shows that ad hoc assumptions for choice of matrix are not justified. *BMC Evol. Biol.* 2006; 6:29. [PubMed: 16563161]
48. Ronquist F, et al. MrBayes 3.2: efficient Bayesian phylogenetic inference and model choice across a large model space. *Syst. Biol.* 2012; 61:539–542. [PubMed: 22357727]
49. Storey JD, Tibshirani R. Statistical significance for genomewide studies. *Proc. Natl. Acad. Sci. USA.* 2003; 100:9440–9445. [PubMed: 12883005]
50. Goldberg JM, et al. The dictyostelium kinome--analysis of the protein kinases from a simple model organism. *PLoS Genet.* 2006; 2:e38. [PubMed: 16596165]
51. Hanks SK, Hunter T, Protein kinases 6. The eukaryotic protein kinase superfamily: kinase (catalytic) domain structure and classification. *FASEB J.* 1995; 9:576–596. [PubMed: 7768349]
52. Manning G, Whyte DB, Martinez R, Hunter T, Sudarsanam S. The protein kinase complement of the human genome. *Science.* 2002; 298:1912–1934. [PubMed: 12471243]
53. Karp PD, et al. Pathway Tools version 13.0: integrated software for pathway/genome informatics and systems biology. *Brief. Bioinform.* 2010; 11:40–79. [PubMed: 19955237]
54. Arakaki AK, Huang Y, Skolnick J. EFICAZ2: enzyme function inference by a combined approach enhanced by machine learning. *BMC Bioinformatics.* 2009; 10:107. [PubMed: 19361344]
55. Karp PD, et al. Expansion of the BioCyc collection of pathway/genome databases to 160 genomes. *Nucleic Acids Res.* 2005; 33:6083–6089. [PubMed: 16246909]
56. Caspi R, et al. The MetaCyc database of metabolic pathways and enzymes and the BioCyc collection of pathway/genome databases. *Nucleic Acids Res.* 2012; 40:D742–D753. [PubMed: 22102576]

Editorial Summary: Thomas Nutman and colleagues report the draft genome of the filarial pathogen *Loa loa*, the African eyeworm. They also report coverage of two other filarial pathogens, *Wuchereria bancrofti* and *Onchocerca volvulus*. Unlike most filariae, *Loa loa* lacks an obligate intracellular *Wolbachia* endosymbiont, and comparative genomic analyses suggest that the *Loa loa* genome does not contain novel metabolic synthesis or transport pathways compared to other filariae.

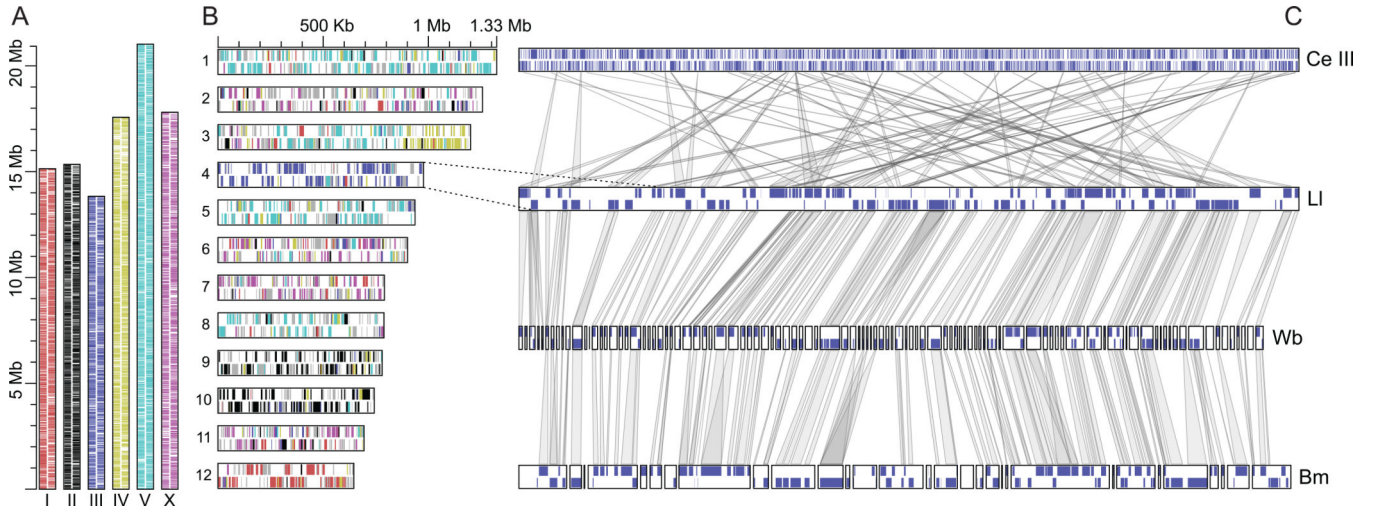


Figure 1. Synteny between filarial worms and *C. elegans*. **(A)** Gene distribution on the *C. elegans* genome. Black-edged vertical bars represent each one of the six *C. elegans* chromosomes, labeled accordingly in the bottommost part of the panel. Horizontal colored boxes within each bar indicate the location and strand of *C. elegans* genes (leftmost column = plus strand; rightmost column = minus strand). The color of the lines designates each chromosome and serves as a color-based legend for panel B; **(B)** Gene distribution on the twelve longest *L. loa* scaffolds. Scaffolds are represented by black-edged horizontal bars, and identified by labels on the left. Vertical colored boxes indicate the position and strand of each gene (uppermost column = plus strand; bottommost column = minus strand). The color-coding indicates the chromosome where each respective ortholog in *C. elegans* is located. Grey colored boxes represent either genes without orthologs in *C. elegans* or genes with two or more homologs in distinct *C. elegans* chromosomes; **(C)** Distribution of *L. loa* scaffold 4 orthologs on the *C. elegans* *W. bancrofti* and *B. malayi* genomes. The scaffolds and chromosomes with best matches to *L. loa* scaffold 4 based on whole genome alignment are depicted here. Each row contains one or more black-edged horizontal bars representing either chromosomes (*C. elegans*) or scaffolds (*L. loa* *B. malayi* and *W. bancrofti*) from each sequenced genome. Purple boxes indicate position and strand of genes. Grey projections connect orthologous genes across organisms.

Author Manuscript

Author Manuscript

Author Manuscript

Author Manuscript

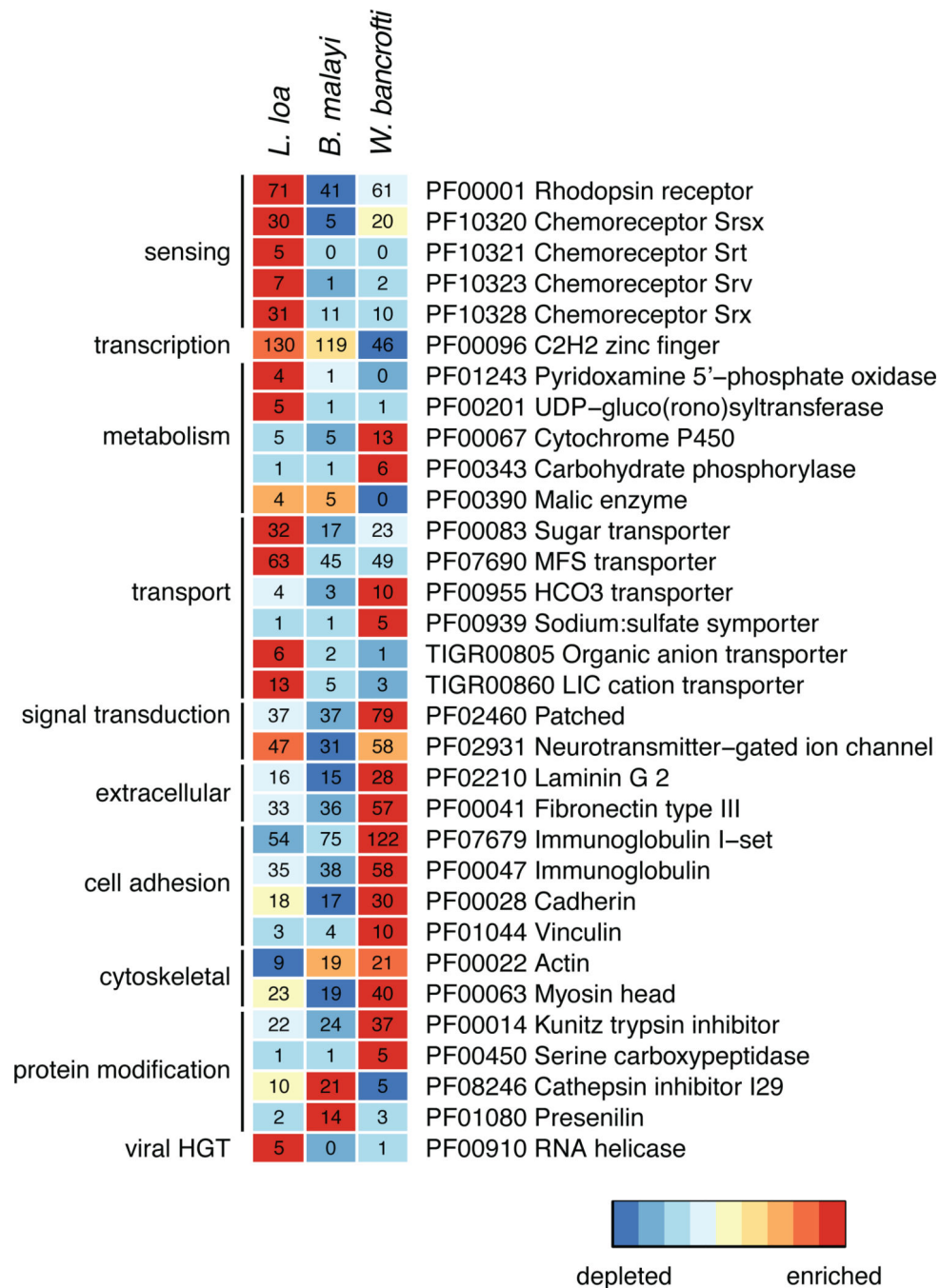


Figure 2.

Enriched and depleted PFAM and TIGRfam domains in each filarial genome relative to the other two. All domains significantly enriched ($p < 0.05$, Fisher's exact test) are shown; red indicates enriched while blue indicates depleted. Numbers of identified domains are given in each box. Broad functional categories representing each domain are shown to the left.

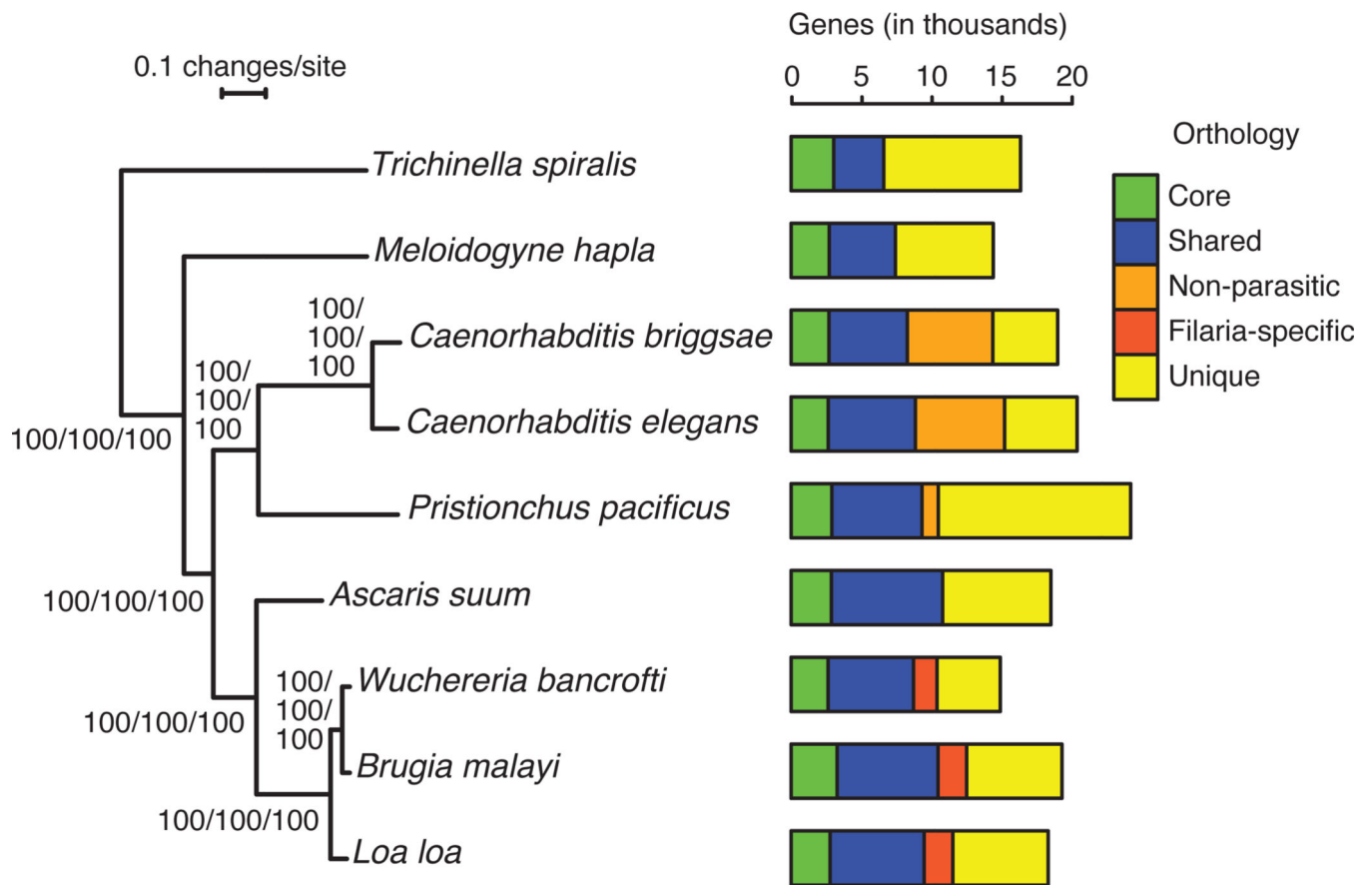


Figure 3. Phylogenomic analysis of nematodes. Maximum likelihood, parsimony, and Bayesian methods all estimated an identical phylogeny using the concatenated protein sequences of 921 single copy orthologs. Adjacent to each node are likelihood bootstrap support values/parsimony bootstrap support values/Bayesian posterior probabilities. The distribution of genes in ortholog clusters is shown to the right of the phylogeny. Core genes are encoded by all genomes, shared genes are encoded by at least two but fewer than all genomes, and unique genes are found only in one genome. Orthologs specific to the non-parasitic nematodes (*C. elegans*, *C. briggsae*, and *P. pacificus*) and filarial nematodes are also highlighted. Of the 6,280 *L. loa* genes with no functional assignment, 3,665 are unique to *L. loa* and 1,158 are filaria-specific.

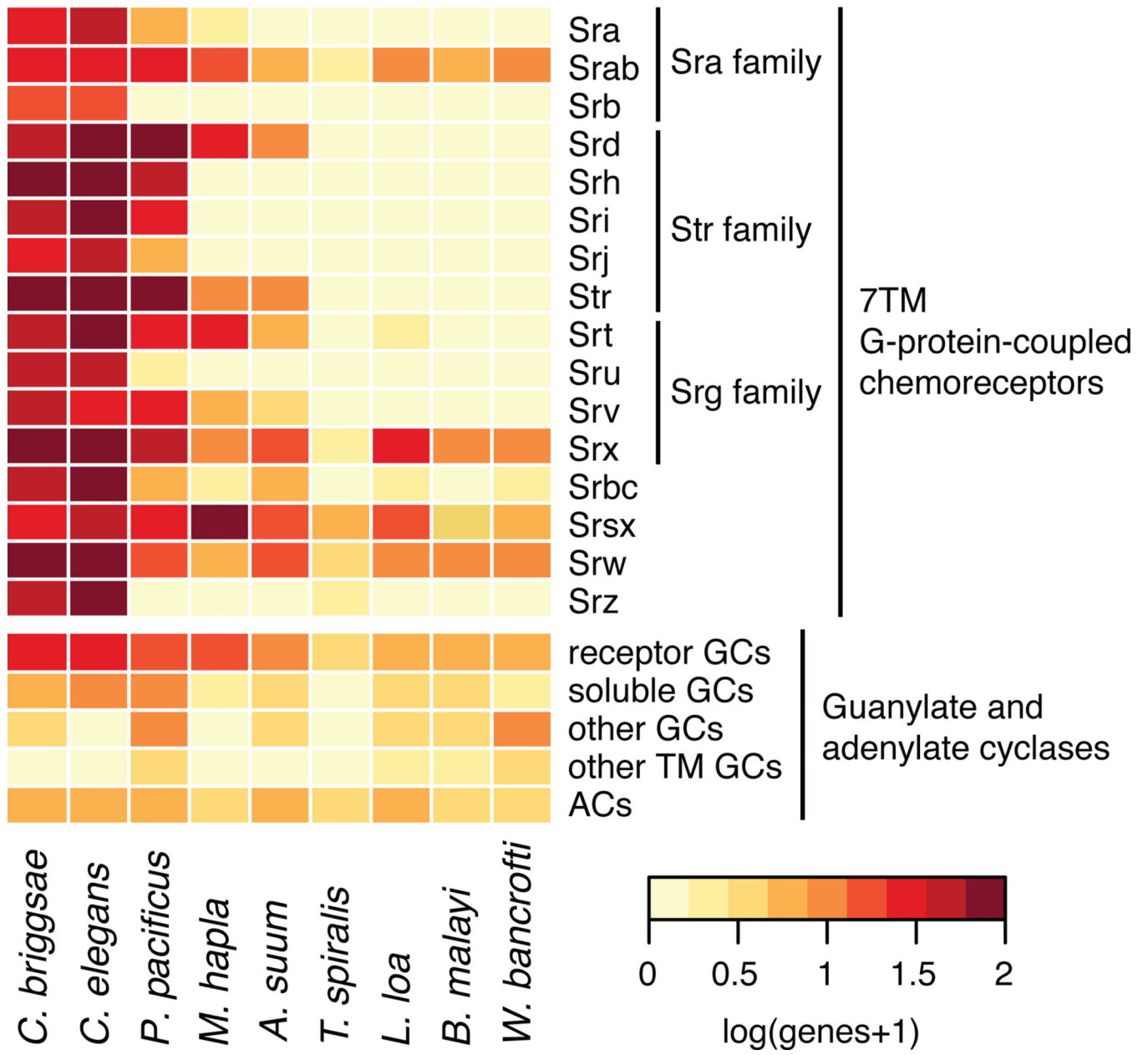


Figure 4. Phylogenetic profile of chemoreceptors in nematode genomes. Both the 7 transmembrane domain G-protein-coupled chemoreceptors (GPCRs) and guanylate and adenylate cyclases are shown.

Table 1

Genome features of filarial worms and their *Wolbachia* endosymbionts; *Wolbachia* genome abbreviations stand for *Wolbachia* of *B. malayi* (*wBm*), *Wolbachia* of *W. bancrofti* (*wWb*), and *Wolbachia* of *O. volvulus* (*wOv*).

Organism	Coverage	Sequence (Mb)	Scaffolds	Scaffold N50 (Kb)	% GC	% Repetitive	% Low Complexity	# of Genes
<i>L. loa</i>	20x	91.4	5774	172	31.0	9.3	1.7	14907 ^a
<i>W. bancrofti</i>	12x	81.5	25884	5.16	29.7	6.2	3.9	19327 ^a
<i>O. volvulus</i>	5x	26.0	22675	1.27	32.5	--	--	--
<i>B. malayi</i>	9x	93.7	8180	94	30.2	12.1	1.1	18348
<i>wBm</i>	11x	1.08	1	--	34.2	--	--	805
<i>wWb</i>	2x	1.05	763	1.62	34.0	--	--	--
<i>wOv</i>	2x	0.44	341	1.51	32.8	--	--	--

^aDue to fragmentation of the genome assemblies, the true *W. bancrofti* gene count is estimated to be 14,496–15,075 genes, while the true *L. loa* gene count is estimated to be 14,261 genes (Supplementary Note).

Table 2

Phylogenetic profiles of biosynthesis pathways hypothesized to be involved in the Filaria-*Wolbachia* symbiosis. Conservation each pathway across nematodes and *Wolbachia* are shown in Supplementary Tables 24 and 25, respectively. Pathways are labeled as complete (+), partial (+/-), or absent (-); *Wolbachia* genome abbreviations stand for *Wolbachia* of *B. malayi* (*wBm*), *Wolbachia* of *D. melanogaster* (*wMel*), *Wolbachia* of *C. pipiens* (*wPip*) and *Wolbachia* of *W. bancrofti* (*wWb*).

Biosynthesis Pathway	<i>C. elegans</i>	<i>C. briggsae</i>	<i>P. pacificus</i>	<i>M. hapla</i>	<i>T. spiralis</i>	<i>A. suum</i>	<i>B. malayi</i>	<i>W. bancrofti</i>	<i>L. loa</i>	<i>wBm</i>	<i>wMel</i>	<i>wPip</i>	<i>wWb</i>
Heme	-	-	-	-	-	-	- ^a	- ^a	- ^a	+	+	+	+
Riboflavin	-	-	-	-	-	-	-	-	-	+	+	+	+
FAD	+	+	+/-	+/-	+	+	+	+	+	+	+	+	+/-
Glutathione	+	+	+	+	+	+	+	+	+	+	+	+	+
Purines	+	+	-	-	+/-	+	-	-	-	+	+	+	+
Pyrimidines	+	+	+	+	+/-	+	+/-	+/-	+/-	+	+	+	+

^a all filarial worms encode a ferrochelatase, the last enzyme in heme synthesis (Supplementary Note).